Eur. Phys. J. Special Topics **185**, 45–55 (2010)

DOI: 10.1140/epjst/e2010-01237-8

THE EUROPEAN PHYSICAL JOURNAL SPECIAL TOPICS

Regular Article

Freak waves in crossing seas

M. Onorato[1,a], D. Proment[1,3], and A. Toffoli[2]

[1] Dipartimento di Fisica Generale, Università di Torino, via P. Giuria 1, 10125 Torino, Italy
[2] Swinburne University of Technology, PO Box 218, Hawthorn, Victoria 3122, Australia
[3] INFN, Sezione di Torino, V.P. Giuria 1, 10125 Torino, Italy

Received in final form and accepted 15 June 2010
Published online 23 August 2010

Abstract. We consider the modulational instability in crossing seas as a potential mechanism for the formation of freak waves. The problem is discussed in terms of a system of two coupled Nonlinear Schröedinger equations. The asymptotic validity of such system is discussed. For some specific angles between the two wave trains, the equations reduce to an integrable system. A stability analysis of these equations is discussed. Furthermore, we present an analytical study of the maximum amplification factor for an unstable plane wave solution. Results indicate that angles between 10° and 30° are the most probable for establishing a freak wave sea. We show that the theoretical expectations are consistent with numerical simulations of the Euler equations.

1 Introduction

The occurrence of freak or rogue waves on the ocean surface represents a serious threat for marine structures and operations due to the large forces that can be released [1]. The research on extreme waves in the ocean has been rapidly developing in the last 10 years and has attracted the attention of many other fields in physics. Recently, rogue waves have been discussed in optical systems, see for example [2,3], in acoustic turbulence in superfluid helium [4], in matter waves (Bose-Einstein condensate) [5] and in nonlinear lattices [6].

In the present paper we will consider only ocean waves in deep water (for a review on oceanic freak waves see [7–9]). In such a context we recall that if a standard spectral analysis of any time series of a wind wave record is performed, it will be found that the square of the Fourier amplitudes as a function of frequencies are well described by the JONSWAP parametrization and the Fourier phases are distributed uniformly in the interval $[0, 2\pi)$. Even though the phases appear as random, some phase locking in between modes cannot be excluded due to the nonlinearity of the governing equations (phase correlation in broad band spectra are difficult to be detected and at the moment there is not a unique satisfactory way of extrecting such information from a time series).

Deep water ocean waves do not consist of a single wave packet; indeed, it has been shown that long crested waves are unstable to transverse perturbation in deep water; therefore any hypothetical infinitely long crested wave is destinated to become a short crested wave after some wave periods, and, as a consequence, the spectrum will become directional. Having this in mind, the relevant question concerning freak waves is the following: how, and how frequent, can a freak wave appear in an ocean whose surface elevation is described by a directional JONSWAP spectrum with random phases? Before trying to answer such a question, it is desirable to discuss the definition of a freak wave. Many authors define a freak wave as a wave whose

[a] e-mail: miguel.onorato@unito.it

height is larger than 2 times the significant wave height. With such a definition many different mechanisms can be responsible for its formation. Clearly, the classical linear superpostion of waves is the first candidate; as just previously mentioned, for random phases and narrow spectra, it is straightforward to calculate the probability of occurence of such large waves. It turns out that 1 wave out of 2980 is larger than 2 times the significant wave height or 8 times the standard deviation of the distribution of the wave amplitudes. Note that such distribution is still described by a Normal shaped due to the Central Limit Theorem. Therefore, the fourth order moment of the surface elevation, the kurtosis, is equal to 3.

In the absence of an ambient current, waves larger than 2 times the significant wave height can be the result of the Benjamin-Feir or modulational instability [10,11] (see also [12]). Such instability is described, at the leading order, by the nonlinear Schrödinger equation [11] assuming potential flow, weakly nonlinearity and quasi-monochromatic waves. In a random wave field, theoretical [13], numerical [14] and experimental [15] studies demonstrated that the modulational instability is responsible for a substantial increase of the probability of occurrence of freak waves, provided the wave field is sufficiently steep and narrow banded, i.e., the spectral energy is concentrated over a restricted range of frequencies and directions. Experimental data recorded in a 270-metre long wave flume (wave tank facility at Marintek, Norway) showed that for some spectral condition the probabily of finding a freak wave is 1/630 [15] (5 times larger that the linear prediction). Note that, in contrast to the linear superposition, the surface amplitudes are not described any more by a Normal distribution; the maximum value of the kurtosis estimated from Marintek data is 4.1. However, one should keep in mind that such experimental and theorethical results have been achieved for long crested waves. Numerical simulations [16,17] and laboratory experiments in a directional wave tank [18–20] have shown that the percentage of freak waves decreases as the directional distribution of the spectrum increases. This result open some questions on the relevance of the modulational instability for the formation of extreme waves. However, the directional properties of the ocean are still far from been completly understood and it is not clear yet how narrow can an ocean wave spectrum be.

Most of the investigations in the past have been conducted for the case of unimodal spectral conditions, i.e. the wave energy is confined around one spectral peak. Very often, however, the wave field in the ocean can be more complicated by the coexistence of two (and sometimes more) wave systems with different directions of propagation. This condition, which is commonly known as a crossing or combined sea, implies that the energy is concentrated over two distinctive spectral peaks. Interestingly enough, the analysis of a number of ship accidents reported as being due to bad weather conditions [21] indicated that a large percentage of accidents might have occurred in the presence of two non-collinear systems, namely a wind sea (wind generated waves) and a swell (waves no longer under the influence of the wind). Synthetic aperture radar (SAR) imagettes suggest that the famous New Year wave, a 26 m-height wave recorded at the Draupner oil field on January 1st 1995 [22], occurred in crossing sea conditions [23]. In combined sea states, it was suggested in [24] that a coexisting swell may grow at the expense of the wind sea. From a theoretical point of view, the modulational instability in crossing seas has been studied using a system of coupled Nonlinear Schröedinger equations (see for example [25–27]). A linear stability analysis of the plane wave solution of the system indicated that the introduction of a second non-collinear wave system can result in an increase of the growth rates of the perturbation and enlargement of the instability region. It was found that the growth rates depend not only on the length of the perturbation and on the steepness of the initial waves, but also on the angle between the two wave systems.

In the present paper, besides presenting a detailed derivation of the coupled NLS equations and a discussion of the coefficients in front of the dispersive and nonlinear terms, we discuss the amplification factor of the plane wave solution of the system in the limit of small perturbations for the case of two equal envelopes traveling at an angle. In the last section we also show, using a higher order spectral method for solving the potential Euler equations, some numerical simulations in crossing seas characterized by an initial condition of two Jonswap spectra and traveling along two different directions of propagation.

2 Derivation of the CNLS equations

Even though the system of CNLS for water waves has been discussed recently in a number of papers [25–28], here we present a detailed derivation which allows us to establish properly the physical limitation of the model. Our starting point is the Zakharov equation in $2D+1$:

$$\frac{\partial a_1}{\partial t} + i\omega_1 a_1 = -i\int T_{1,2,3,4} a_2^* a_3 a_4 \delta_{1,2}^{3,4} d\mathbf{k}_{2,3,4}. \tag{1}$$

Here $a_i = a(\mathbf{k}_i, t)$ is the complex variable defined for example in [29], $\delta_{1,2}^{3,4} = \delta(\mathbf{k}_1+\mathbf{k}_2-\mathbf{k}_3-\mathbf{k}_4)$ and $\omega = \sqrt{g\kappa}$, where κ is the modulus of the vector $\mathbf{k}$. We work under the hypothesis that the energy is concentrated mainly around two carriers waves, therefore it is natural to consider the following decomposition:

$$a(\mathbf{k}) = A(\mathbf{k}-\mathbf{k}^{(a)})e^{-i\omega^{(a)}t} + B(\mathbf{k}-\mathbf{k}^{(b)})e^{-i\omega^{(b)}t} \tag{2}$$

with $\mathbf{k}^{(a)} = (k^{(a)}, l^{(a)})$, $\mathbf{k}^{(b)} = (k^{(b)}, l^{(b)})$, $\omega^{(a)} = \sqrt{g|\mathbf{k}^{(a)}|}$ and $\omega^{(b)} = \sqrt{g|\mathbf{k}^{(b)}|}$. Inserting (2) into (1), after some algebra, it is straightforward to obtain the following equations:

$$\begin{aligned}\frac{\partial A_1}{\partial t} + i(\omega_1-\omega^{(a)})A_1 = &-i\int T_{1,2,3,4}(A_2^*A_3A_4 + 2B_2^*B_3A_4)\delta_{1,2}^{3,4}d\mathbf{k}_{2,3,4}\\ &+ie^{-i(\omega^{(a)}-\omega^{(b)})t}\int T_{1,2,3,4}B_2^*A_3A_4\delta_{1,2}^{3,4}d\mathbf{k}_{2,3,4}\end{aligned} \tag{3}$$

$$\begin{aligned}\frac{\partial B_1}{\partial t} + i(\omega_1-\omega^{(b)})B_1 = &-i\int T_{1,2,3,4}(B_2^*B_3B_4 + 2A_2^*A_3B_4)\delta_{1,2}^{3,4}d\mathbf{k}_{2,3,4}\\ &+ie^{-i(\omega^{(b)}-\omega^{(a)})t}\int T_{1,2,3,4}A_2^*B_3B_4\delta_{1,2}^{3,4}d\mathbf{k}_{2,3,4}\end{aligned} \tag{4}$$

where now $A_i = A(\mathbf{k}_i - \mathbf{k}^{(a)})$ and $B_i = B(\mathbf{k}_i - \mathbf{k}^{(b)})$. We recall that the nonlinear time scale in the Zakharov equation is $\tau_{NL} \sim 1/(\epsilon^2\omega)$, where ϵ is the wave steepness. The last term in both equations oscillate with an angular frequency $\Delta\Omega = \omega^{(\mathrm{b})} - \omega^{(\mathrm{a})}$. If $\Delta\Omega \sim \epsilon^2\omega^{(\mathrm{a})}$, i.e. $\omega^{(b)} \sim \omega^{(a)}$ the terms oscillate with a frequency corresponding to the nonlinear time scale τ_{NL} and their contribution cannot be neglected in both equations. However, if the $\omega^{(b)}$ and $\omega^{(a)}$ are different, then these terms result in fast oscillations that, on average, do not give any contribution to the wave evolution and can be safely neglected in the equations.

We consider the particular case of $\mathbf{k}^{(a)} = (k, l)$ and $\mathbf{k}^{(b)} = (k, -l)$ with $l \neq 0$ (so that the oscillating terms can be neglected) and consider each wave system as quasi-monochromatic. A Taylor expansion of the dispersion relation around $\mathbf{k}^{(a)}$ leads to:

$$\begin{aligned}\omega(\kappa) - \omega^{(a)} = &\frac{\partial\omega}{\partial k_x}(k_x-k) + \frac{\partial\omega}{\partial k_y}(k_y-l) + \frac{1}{2}\frac{\partial^2\omega}{\partial k_x^2}(k_x-k)^2\\ &+\frac{1}{2}\frac{\partial^2\omega}{\partial k_y^2}(k_y-l)^2 + \frac{\partial^2\omega}{\partial k_x\partial k_y}(k_x-k)(k_y-l) + \ldots\end{aligned} \tag{5}$$

Similarly the expansion can be done around $\mathbf{k}^{(b)} = (k, -l)$. In order to balance nonlinearity and dispersion, we consider only the expansion to the leading order of the coupling coefficient. We obtain the following two coefficients:

$$\xi = T(\mathbf{k}^{(a)}, \mathbf{k}^{(a)}, \mathbf{k}^{(a)}, \mathbf{k}^{(a)}) = T(\mathbf{k}^{(b)}, \mathbf{k}^{(b)}, \mathbf{k}^{(b)}, \mathbf{k}^{(b)}) = \kappa^3 \tag{6}$$

$$\zeta = T(\mathbf{k}^{(a)}, \mathbf{k}^{(b)}, \mathbf{k}^{(b)}, \mathbf{k}^{(a)}) = \frac{k^5 - k^3l^2 - 3kl^4 - 2k^4\kappa + 2k^2l^2\kappa + 2l^4\kappa}{-2k^2 - 2l^2 + k\kappa}, \tag{7}$$

where $\kappa = \sqrt{k^2 + l^2}$. Equations (3) and (4) becomes:

$$\frac{\partial A_1}{\partial t} + i(C_x^{(a)}\chi_x + C_{ya}^{(a)}\chi_x + \alpha^{(a)}\chi_x^2 + \beta^{(a)}\chi_{ya}^2 + \gamma^{(a)}\chi_x\chi_{ya})A_1 = \\ -i\int(\xi A_2^* A_3 A_4 + 2\zeta B_2^* B_3 A_4)\delta_{1,2}^{3,4} d\mathbf{k}_{2,3,4} \tag{8}$$

$$\frac{\partial B_1}{\partial t} + i(C_x^{(b)}\chi_x + C_{yb}^{(b)}\chi_x + \alpha^{(b)}\chi_x^2 + \beta^{(b)}\chi_{yb}^2 + \gamma^{(b)}\chi_x\chi_{yb})B_1 = \\ -i\int(\xi B_2^* B_3 V_4 + 2\zeta A_2^* A_3 B_4)\delta_{1,2}^{3,4} d\mathbf{k}_{2,3,4} \tag{9}$$

where $\chi_x = k_x - k$, $\chi_{ya} = k_y - l$ and $\chi_{yb} = k_y + l$. The coefficients are defined as follows:

$$\begin{aligned} C_x &= C_x^{(a)} = C_x^{(b)} = \frac{\omega(\kappa)}{2\kappa^2}k \\ C_y &= C_y^{(a)} = -C_y^{(b)} = \frac{\omega(\kappa)}{2\kappa^2}l \\ \alpha &= \alpha^{(a)} = \alpha^{(b)} = \frac{\omega(\kappa)}{8\kappa^4}(2l^2 - k^2) \\ \beta &= \beta^{(a)} = \beta^{(b)} = \frac{\omega(\kappa)}{8\kappa^4}(2k^2 - l^2) \\ \gamma &= \gamma^{(a)} = -\gamma^{(b)} = -\frac{3\omega(\kappa)}{4\kappa^4}lk. \end{aligned} \tag{10}$$

Using the Fourier Transform, we obtain:

$$\frac{\partial A}{\partial t} + C_x\frac{\partial A}{\partial x} + C_y\frac{\partial A}{\partial y} - i\alpha\frac{\partial^2 A}{\partial x^2} - i\beta\frac{\partial^2 A}{\partial y^2} + i\gamma\frac{\partial^2 A}{\partial x\partial y} + i(\xi|A|^2 + 2\zeta|B|^2)A = 0 \tag{11}$$

$$\frac{\partial B}{\partial t} + C_x\frac{\partial B}{\partial x} - C_y\frac{\partial B}{\partial y} - i\alpha\frac{\partial^2 B}{\partial x^2} - i\beta\frac{\partial^2 B}{\partial y^2} - i\gamma\frac{\partial^2 B}{\partial x\partial y} + i(\xi|B|^2 + 2\zeta|A|^2)B = 0. \tag{12}$$

Note that usually the NLS equation is written in variables that have the dimensions of a surface elevation. Hence, it is custom to consider the following new complex amplitudes A' and B':

$$A' = \left[\frac{2\kappa}{\omega(\kappa)}\right]^{1/2} A, \qquad B' = \left[\frac{2\kappa}{\omega(\kappa)}\right]^{1/2} B. \tag{13}$$

The equations then become:

$$\frac{\partial A}{\partial t} + C_x\frac{\partial A}{\partial x} + C_y\frac{\partial A}{\partial y} - i\alpha\frac{\partial^2 A}{\partial x^2} - i\beta\frac{\partial^2 A}{\partial y^2} + i\gamma\frac{\partial^2 A}{\partial x\partial y} + i(\xi'|A|^2 + 2\zeta'|B|^2)A = 0 \tag{14}$$

$$\frac{\partial B}{\partial t} + C_x\frac{\partial B}{\partial x} - C_y\frac{\partial B}{\partial y} - i\alpha\frac{\partial^2 B}{\partial x^2} - i\beta\frac{\partial^2 B}{\partial y^2} - i\gamma\frac{\partial^2 B}{\partial x\partial y} + i(\xi'|B|^2 + 2\zeta'|A|^2)B = 0 \tag{15}$$

where the primes in A and B have been omitted for brevity. The surface elevation $\eta(x, y, t)$ is related to such wave envelope to the leading order in the following way:

$$\eta = \frac{1}{2}(Ae^{i(kx+ly-\omega t)} + Be^{i(kx-ly-\omega t)}) + c.c. \tag{16}$$

where c.c. stands for complex conjugate. The new coefficients are given by:

$$\begin{aligned} \xi' &= \frac{\omega(\kappa)}{2\kappa}\xi = \frac{1}{2}\omega(\kappa)\kappa^2 \\ \zeta' &= \frac{\omega(\kappa)}{2\kappa}\zeta = \frac{\omega(\kappa)}{2\kappa}\left(\frac{k^5 - k^3l^2 - 3kl^4 - 2k^4\kappa + 2k^2l^2\kappa + 2l^4\kappa}{-2k^2 - 2l^2 + k\kappa}\right). \end{aligned} \tag{17}$$

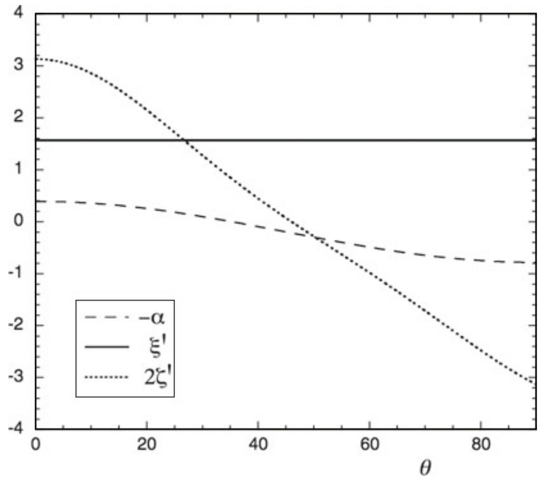

Fig. 1. Coefficients of the CNLS equations as a function of θ.

It is easy to show that if $A = B$ and $l = 0$ the equation for the variable $A + B$ is not the correct NLS equation for a single wave train; this is due to the fact that, as mentioned before, the coupled system is not asymptotically valid for $l = 0$. In order to re-derive the single NLS equation the oscillating terms previously neglected should be included.

2.1 Asymptotic validity of the system of equations

The single NLS equation is derived by assuming that the time scale of the dispersion is of the same order as the time scale of the nonlinearity. Formally, it is derived by introducing a slow variables $\tau = \epsilon^2 t$, $x' = \epsilon x$ and a coordinate system moving with the group velocity. For the system (14)–(15), the situation is more complicated because the group velocities along the y coordinate are different unless $l = 0$ (such a case should, however, be excluded because of the assumptions previously made). The system (14)–(15) is not asymptotically valid because the dispersive and nonlinear terms are not in balance with time. In other words, the time scale of the nonlinearity is not the same as the time scale of dispersion.

Strictly speaking the system is valid only along the direction at which the group velocities are the same. This corresponds to the following set of NLS equations:

$$\frac{\partial A}{\partial t} - i\alpha\frac{\partial^2 A}{\partial x^2} + i(\xi'|A|^2 + 2\zeta'|B|^2)A = 0 \tag{18}$$

$$\frac{\partial B}{\partial t} - i\alpha\frac{\partial^2 B}{\partial x^2} + i(\xi'|B|^2 + 2\zeta'|A|^2)B = 0. \tag{19}$$

3 Analysis of the coefficients in the CNLS equations

In [14] a simple parameter (nowadays known as the Benjamin-Feir index) based on the ratio between nonlinearity and dispersion has been found to be useful for establishing the sea states in which freak waves develop more frequently. Therefore, one simple way of getting some indications on the most favorable angle for the formation of freak waves in the coupled NLS system consists in analyzing the coefficients in front of the dispersive, self-interaction and cross-interaction term, respectively α, ξ' and $2\zeta'$. In Fig. 1 we show the coefficients $-\alpha$, ξ' and $2\zeta'$ as a function of the angle $\theta = \arctan(l/k)$ (without loss of generality we have fixed $\kappa = 1\ m^{-1}$). As

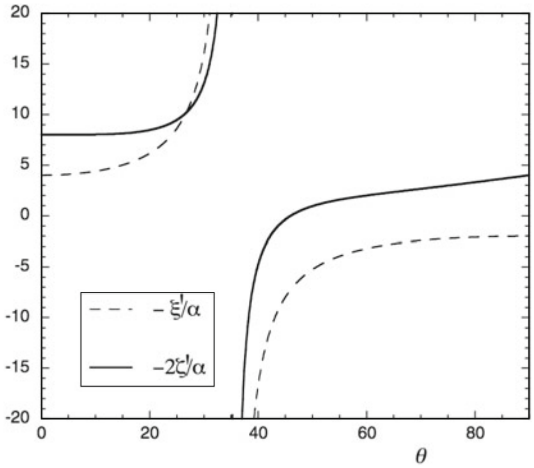

Fig. 2. Ratio between nonlinear and dispersive coefficients as a function of θ.

it was previously noted in [25] $-\alpha$ changes sign at $\theta = \theta_c \simeq 35.264°$ from positive to negative. This, as will be seen in the next section, has some consequences on the stability properties of the solutions of the system. The coefficient ξ' is independent of the angle θ, while ζ change sign at $\theta \simeq 46.017°$.

In order to estimate the relative relevance of the nonlinear terms for different angles, we present the ratios ξ'/α and $2\zeta'/\alpha$ as a function of θ in Fig. 2: both curves have a vertical asymptote for $\theta = \theta_c$. For values around such angle the nonlinear terms are much bigger than the linear ones, therefore it would be expected that freak waves can develop in such conditions. Strictly speaking, the system is not valid anymore around $\theta = \theta_c$; this is because the spirit under which the system has been derived is that the time scale of the nonlinearity and dispersion are the same. For $\theta = \theta_c$, it is necessary to include a higher order dispersive term in the equations. By expanding the dispersion relation to third order, we obtain the following equations:

$$\frac{\partial A}{\partial t} - \mu \frac{\partial^3 A}{\partial x^3} + i(\xi'|A|^2 + 2\zeta'|B|^2)A = 0 \tag{20}$$

$$\frac{\partial B}{\partial t} - \mu \frac{\partial^3 B}{\partial x^3} + i(\xi'|B|^2 + 2\zeta'|A|^2)B = 0 \tag{21}$$

where

$$\mu = \frac{3\omega(\kappa)}{8}\left(\frac{k^3 - 6kl^2}{8\kappa^6}\right). \tag{22}$$

The stability properties of such a system will be investigated elsewhere.

In Fig. 3 we show the absolute value of the ratio between the coefficients of the nonlinear term: the nonlinearity due to the cross-interaction term dominates for angles less than $\theta = \theta_{int} = 26.732°$. For such an angle the coefficients in front of the nonlinear terms are identical. Therefore, the CNLS equations (18) and (19) reduce to the Manakov system which is known to be integrable in terms of the Inverse Scattering Transform. This is an interesting remark because for such specific angle all solutions of (18) and (19) can in principle be obtained. For angle larger than θ_{int} the self-interaction nonlinearity dominates. For $\theta = 46.017^0$, as previously noted, the cross-interaction term vanishes and the system becomes uncoupled; again this corresponds to an integrable condition.

To summarize we can state the followings:

1. for $\theta < 35.3°$, dispersive and nonlinear terms have the same sign. This means that the system is focusing;
2. the ratio between nonlinearity and dispersion becomes larger as θ approaches $35.3°$ (this is valid for both self-interaction and cross-interaction nonlinearity);

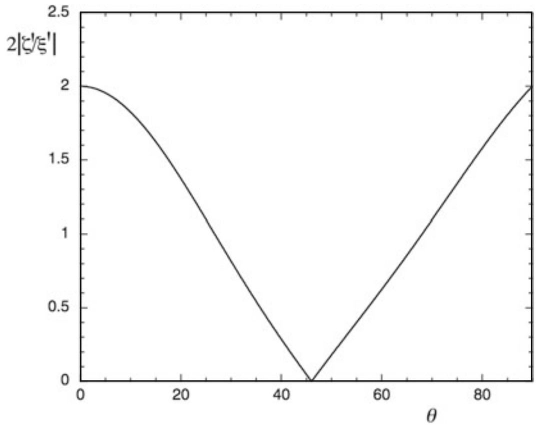

Fig. 3. Ratio between self interaction and cross-interaction coefficients as a function of θ.

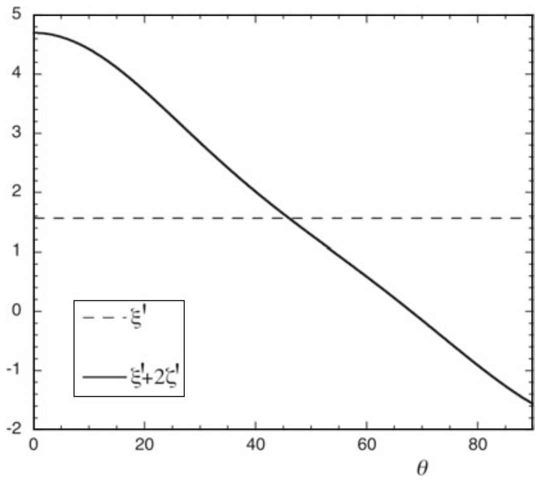

Fig. 4. as a function of θ.

3. the cross-interaction nonlinearity is stronger than the self interaction one for angles between 0 and 26.732°;
4. for some specific angles, $\theta = 46.017°$ and 26.732° the system is integrable.

4 A simpler model

In order to investigate analytically the system, we make the hypothesis that at time $t = 0$ the envelope A and B are equal. Even though the envelopes are the same, still the two carrier waves travel in different directions. A trivial remark is that in such condition, due to the symmetry of the equations (18) and (19), A will be equal to B for all times. This basically means that the equation relevant for the dynamics is:

$$\frac{\partial A}{\partial t} - i\alpha \frac{\partial^2 A}{\partial x^2} + i\nu |A|^2 A = 0 \tag{23}$$

where $\nu = \xi' + 2\zeta'$ is the standard NLS, i.e. an integrable equation. In figure 4 we show the coefficient of the self interaction term ξ' and ν as a function of θ. Up to $\theta = 46.017°$, ν is larger than ξ'. For larger angles the nonlinearity is larger for an uncoupled system.

It is well known that equation (23) has analytical unstable solutions [30]. For a plane wave solution with a small perturbation at time $t = -\infty$, it is possible to show that the maximum

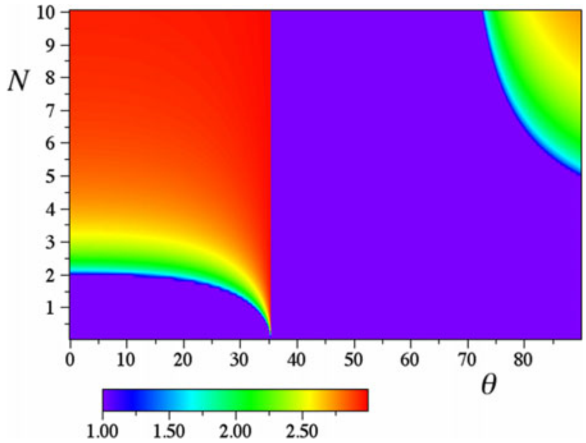

Fig. 5. Amplification factor as a function of θ and N.

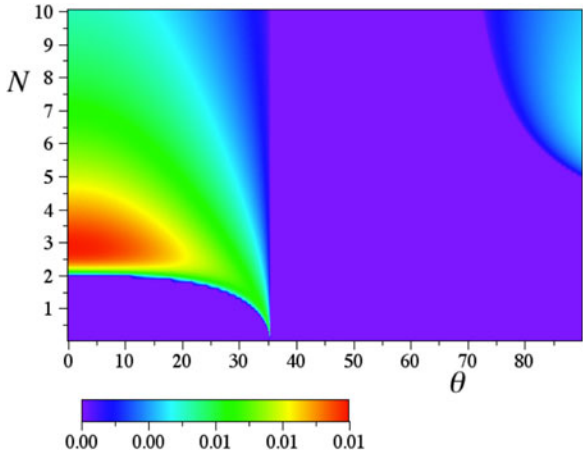

Fig. 6. Growth rate as a function of θ and N.

amplification factor for the Akhmediev breather solution has the following form:

$$\frac{A_{max}}{A_0} = 1 + 2\sqrt{1 - \left[\sqrt{\frac{\alpha}{2\nu}}\frac{\kappa^2}{\epsilon N}\right]^2} \tag{24}$$

where $\epsilon = A_0\kappa$ and N is the number of waves under the perturbation. In Fig. 5 we plot A_{max}/A_0 as a function of N and θ. The steepness considered for the plot is $\epsilon = 0.1$. The colors in the figure indicate different amplification factors. For small amplitude perturbations of a plane wave solution, the maximum amplification is equal to 3. This value is reached for angles approaching θ_c and for large number of waves under the perturbation (large N). Note that there exists also a region of amplification for angles larger than $\theta > 68.028°$. In [25] the linear stability analysis of a plane wave solution of system (18) and (19) has been derived. Here, in light of the analysis performed on the coefficients and on the amplification factor, we discuss the growth rate of small perturbations on plane wave solutions with equal amplitudes. In Fig. 6, we show the normalized growth rate $\Omega' = \Omega/\omega$ as a function of N and θ for waves of steepness 0.1 each. As previously noted for the amplification factor, there exists a region of instability for large angles and large number of waves. While the boundaries of the region in the $N - \theta$ plane of the amplification factor greater than one and the growth rate greater than zero are the same, the region for maximum amplification factor ($\theta = \theta_c$ and large N) does not correspond to the region of maximum growth rate. As $\theta \to \theta_c$ the growth rate tends to zero; this is also true for

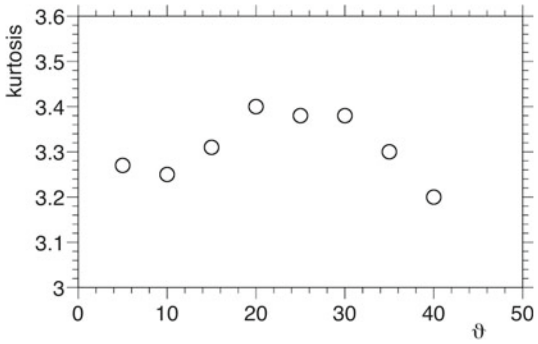

Fig. 7. Maximum of the kurtosis as a function of θ.

large N. The growth rate has a maximum for $N \simeq 3$ and for an angle $\theta = 0$. These values do not correspond necessarely to a large amplification factor. A freak wave is the result of a large amplification factor and, at the same time, a large growth rate. Therefore, we expect to face a freak sea state for angles between about 10° and 30°, which can be considered as a compromise between large growth rates and large amplification factors.

5 Numerical results

The purpose of the following numerical tests is to verify if, in more realistic conditions, the predictions just obtained are somehow reasonable. In this framework, we will present some numerical simulations of two long crested wave systems characterized each by a JONSWAP spectrum with random phases. Numerical simulations have been performed with a higher order approximation of the potential Euler equations for water waves. Assuming an irrotational, inviscid and incompressible fluid flow, the velocity potential $\phi(x, y, z, t)$ satisfies the Laplace's equation everywhere in the fluid. At the bottom ($z = -\infty$) the boundary condition is such that the vertical velocity is zero. At the free surface, $z = \eta(x, y, t)$, the kinematic and dynamic boundary conditions are satisfied for the free surface elevation and the velocity potential at the free surface $\psi(x, y, t) = \phi(x, y, \eta(x, y, t), t)$. Using the free surface variables these boundary conditions have the following form [11]:

$$\psi_t + g\eta + \frac{1}{2}\left(\psi_x^2 + \psi_y^2\right) - \frac{1}{2}W^2\left(1 + \eta_x^2 + \eta_y^2\right) = 0, \tag{25}$$

$$\eta_t + \psi_x\eta_x + \psi_y\eta_y - W\left(1 + \eta_x^2 + \eta_y^2\right) = 0, \tag{26}$$

where $W(x, y, t) = \phi_z|_\eta$ represents the vertical velocity evaluated at the free surface. Numerical simulations of equations (25) and (26) were performed with the Higher Order Spectral Method (HOSM) proposed in [31,32]. This is a pseudo–spectral method that uses a series expansion in the wave slope of the vertical velocity $W(x, y, t)$ about the free surface, in order to estimate the surface elevation and the velocity potential at each time step. The HOSM is not affected by any bandwidth constraints. The initial surface elevation was calculated from two identical JONSWAP spectra (peak period $T_p = 1s$, i.e. wavelength $\lambda_p = 1.56\,m$, significant wave height $H_s = 0.06$ and peak enhancement factor $\gamma = 6$) with mean directions forming angles of $\pm\theta$ with the x direction of propagation, by first switching from (ω, ϑ) to (k_x, k_y) coordinates and then using an inverse Fourier transform with the random amplitude and phase approximation. The velocity potential $\psi(x, y, t = 0)$ was obtained from the input surface with linear theory. The wave field was contained in a square domain of about $20\,m$ with spatial mesh of 256×256 nodes ($\Delta\mathrm{x} = \Delta\mathrm{y} = 0.078\,\mathrm{m}$). Periodic boundary conditions are considered. A fourth-order Runge-Kutta method was used for the time integration. A time step of $\Delta\mathrm{t} = \mathrm{T_p}/100$ was employed in the simulations (details on numerical simulations of the random sea surface with HOSM can be found in e.g. [33–36]). The simulation was performed for angle θ between 0°

and 40° with a interval of 5°. The simulations have been carried out for a time up to $60\,T_p$. About 100 repetitions with the same input spectrum and different random amplitudes and phases have been performed to achieve statistically significant results. The kurtosis has been calculated at each time step for all simulations and its maximum for each simulation is shown in 7. It is interesting to note that for angle larger than 10° the kurtosis starts to increase reaching a value of 3.4. for an angle of about 20°. Then it remains constant up to 30° and after which it decreases. The picture coming out of the simulation is consistent with the predictions described in the previous section. Note that in our theoretical analysis we have considered plane wave solutions traveling at an angle perturbed only along the x direction of propagation. In the present simulations we have two random spectra traveling at an angle without any perturbation imposed. The system simulated is fully two dimensional and it does not preclude any limitation on natural perturbation on the y direction.

6 Conclusions

Freak waves are a rare event on the ocean surface and one of the main problem in establishing their nature is the lack of experimental measurements in the ocean. A conclusive statement on the most probable mechanism that can lead to a formation of a freak waves in the ocean is in our opinion not possible at the moment. There are a number of candidates, each with its own rights.

Here we have discussed a possible mechanism that results from the interaction of two non-collinear wave fields. With respect to the real ocean, our model is surely an oversimplification. Besides the weakly nonlinearity and the narrow band assumptions (which in the past have always lead to reasonable results), we have made the hypothesis that the two wave trains have exactly the same frequency. This is not surely a typical condition that takes place in the ocean where swell and wind seas are characterized by different frequencies. However, our model is a first step towards the understanding of the nonlinear dynamics that takes place when two wave systems overlap. One thing that should be kept in mind is that a large growth rate does not necessarily mean extreme waves (a freak wave may be the result of a modulational instability but not every modulational instability processes result in a freak wave). On the other side large amplification factors may have a small growth rate. Therefore, the appearance of freak waves can be thought as a compromise between large growth rates and large amplification factors.

In the present paper we have investigated the modulational instability for two equal, non-collinear wave systems traveling at an angle θ; we have investigated the dependence of the growth rate and amplification factor from the angle θ. We have found that for some angles the equations reduces to the Manakov system. In general we have found that large amplification factors of small amplitude perturbations of plane wave solutions are observed for angles approaching $\theta = 35.264^o$. For such an angle the dispersive terms turns identically to zero. While the nonlinearity is strong and the amplification factor reaches the maximum value 3, the growth rate is small, therefore the freak wave unlikely will appear. For very large growth rates the amplification factor is small and again freak waves will not appear. Such simple analysis indicates that freak waves may appear with a higher probability for angles between 10° and 30°. This result is consistent with numerical simulations of the Euler equations for random spectra.

The numerical simulations were partially performed by using the K.U. Leuven's High Performance Computing (HPC) facilities. Financial support of the Australian Research Council and Woodside Energy Ltd through the grant LP0883888 is also acknowledged. MO acknowledge funding from EU project EXTREME SEAS, Grant agreement no.: 234175, O.N.R and Army Corp of Engineers. We thank Al Osborne, J. Monbaliu and M. Serio for always fruitful discussions.

References

1. G. Clauss, Appl. Ocean. Res. **24**, 147 (2002)
2. D.R. Solli, C. Ropers, P. Koonath, B. Jalali, Nature **450**, 1054 (2007)

3. A. Montina, U. Bortolozzo, S. Residori, F.T. Arecchi, Phys. Rev. Lett. **103**, 173901 (2009)
4. A.N. Ganshin, V.B. Efimov, G.V. Kolmakov, L.P. Mezhov-Deglin, P.V.E. McClintock, Phys. Rev. Lett. **101**, 065303 (2008)
5. Y.V. Bludov, V.V. Konotop, N. Akhmediev, Phys. Rev. A **80**, 033610 (2009)
6. A. Maluckov, L. Hadzievski, N. Lazarides, G.P. Tsironis, Phys. Rev. E **79** (2009), ISSN 1539-3755
7. C. Kharif, E. Pelinovskij, A. Slunjaev, *Rogue Waves in the Ocean* (Springer, 2009)
8. C. Kharif, E. Pelinovsky, Eur. J. Mech./B Fluids **22**, 603 (2003)
9. K. Dysthe, H.E. Krogstad, P. Müller, Ann. Rev. Fluid Mech. **40**, 287 (2008)
10. T.B. Benjamin, J.E. Feir, J. Fluid Mech. **27**, 417 (1967)
11. V. Zakharov, J. Appl. Mech. Tech. Phys. **9**, 190 (1968)
12. V. Zakharov, A. Dyachenko, A. Prokofiev, Eur. J. Mech./B Fluids **25**, 677 (2006)
13. P.A.E.M. Janssen, J. Phys. Ocean. **33**, 863 (2003)
14. M. Onorato, A. Osborne, M. Serio, S. Bertone, Phys. Rev. Lett. **86**, 5831 (2001)
15. M. Onorato, A. Osborne, M. Serio, L. Cavaleri, C. Brandini, C. Stansberg, Eur. J. Mech. B/Fluids **25**, 586 (2006)
16. M. Onorato, A.R. Osborne, M. Serio, Phys. Fluids **14**, 25 (2002)
17. H. Socquet-Juglard, K. Dysthe, K. Trulsen, H. Krogstad, J. Liu, J. Fluid Mech. **542**, 195 (2005)
18. M. Onorato, L. Cavaleri, S. Fouques, O. Gramdstad, P.A.E.M. Janssen, J. Monbaliu, A.R. Osborne, C. Pakozdi, M. Serio, C. Stansberg, et al., J. Fluid Mech. **627**, 235 (2009)
19. M. Onorato, T. Waseda, A. Toffoli, L. Cavaleri, O. Gramdstad, P.A.E.M. Janssen, K.T., J. Monbaliu, N. Mori, A.R. Osborne, et al., Phys. Rev. Lett. **102** (2009)
20. T. Waseda, T. Kinoshita, H. Tamura, J. Phys. Oceanogr. **39**, 621 (2009)
21. A. Toffoli, J. Lefèvre, E. Bitner-Gregersen, J. Monbaliu, Appl. Ocean Res. **27**, 281 (2005)
22. S. Haver, J. Andersen, Freak waves: rare realizations of a typical population or typical realizations of a rare population?, in *Proc. 10-th Int. Offshore and Polar Engineering (ISOPE) Conf.* (Seattle, USA, 2000)
23. S. Lehner, H. Günther, W. Rosenthal, Extreme wave observations from radar data sets, in *Ocean Waves Measurements and Analysis, Fifth International Symposium WAVES 2005* (Madrid, Spain, 2005), paper 69
24. H. Tamura, T. Waseda, Y. Miyazawa, Geophys. Res. Lett. **36**, 01607 (2009)
25. M. Onorato, A. Osborne, M. Serio, Phys. Rev. Lett. **96**, 014503 (2006)
26. P.K. Shukla, I. Kaurakis, B. Eliasson, M. Marklund, L. Stenflo, Phys. Rev. Lett. **97**, 094501 (2006)
27. A. Gronlund, B. Eliasson, M. Marklund, EPL **86** (2009), ISSN 0295-5075
28. J. Hammack, D. Henderson, H. Segur, J. Fluid Mech. **532**, 1 (2005)
29. V. Krasitskii, J. Fluid Mech. **272** (1994)
30. N. Akhmediev, V. Korneev, Theor. Math. Phys. **69**, 1089 (1986)
31. B.J. West, K.A. Brueckner, R.S. Jand, D.M. Milder, R.L. Milton, J. Geophys. Res. **92**, 11803 (1987)
32. D.G. Dommermuth, D.K. Yue, J. Fluid Mech. **184**, 267 (1987)
33. M. Tanaka, J. Fluid Mech. **444**, 199 (2001)
34. M. Onorato, A.R. Osborne, M. Serio, D. Resio, A. Puskarev, V.E. Zakharov, C. Brandini, Phys. Rev. Lett. **89**, 4.144501 (2002)
35. G. Ducrozet, D. Bonnefoy, D. Le Touzé, P. Ferrant, Nat. Hazards Earth Syst. Sci. **7**, 109 (2007)
36. A. Toffoli, M. Benoit, M. Onorato, E.M. Bitner-Gregersen, Nonlin. Proc. Geophys. **16**, 131 (2009)